

Terahertz Response of Optically Excited Semiconductors

M. Kira, W. Hoyer, and S. W. Koch

Fachbereich Physik, Philipps Universität, Renthof 5, 35032 Marburg/Germany

(Dated: October 29, 2018)

The induced terahertz response of semiconductor systems is investigated with a microscopic theory. In agreement with recent terahertz experiments, the developed theory fully explains the ultrafast build up of the plasmon resonance and the slow formation of incoherent excitonic populations. For incoherent conditions, it is shown that a terahertz field exclusively probes the correlated electron-hole pairs via a symmetry breaking between many-body correlations with even and odd functional form.

PACS numbers: 78.47.+p, 73.20.Mf, 78.67.De

The light-matter coupling of semiconductor systems is usually mediated by the optical polarization generated by band-to-band excitations. This polarization — i.e. the induced coherence between the optically coupled valence and conduction bands — is influenced and modified by already existing or excitation generated populations of quasiparticles. However, since optical methods probing band-to-band transitions cannot directly measure populations, such approaches provide only indirect information about the characteristics of the semiconductor excitations. Usually it is therefore very difficult, if not impossible, to unambiguously attribute the observed changes in the interband optical response to their genuine origin. Hence, to learn about the true nature of optically generated excitations and quasi-particles, one needs supplementary information from other methods. With this respect, recent experimental efforts^{1,2,3,4,5} have extended semiconductor optics toward the regime where transitions between quasi-particle states can be probed directly with far infrared fields at terahertz (THz) frequencies which are orders of magnitude lower than the usual band-to-band transitions. Especially, the combination of interband optical excitation and intraband measurement of the induced THz absorption allowed the experimentalists to discuss seemingly different questions such as the ultrafast build-up of plasma screening⁴ and the formation of excitonic correlations⁵.

To provide a fundamental basis for the analysis of the semiconductor THz response, we develop in this Letter a comprehensive microscopic theory that consistently includes Coulombic many-body interactions, coupling to optical and THz fields as well as lattice vibrations. The developed theory is applied to compute the time-resolved THz response after optical interband excitation and as special cases, we investigate the build up of the plasmon resonance and the gradual formation of exciton population transitions. Our results demonstrate that the incoherent THz response can be attributed to transitions between specific many-body states of the correlated electron-hole pairs, establishing this technique as uniquely qualified to identify the genuine nature and dynamics of these quasi-particle excitations.

In general, the optical response of semiconductors to a classical transversal electric field $E(z, t)$ can be solved from Maxwell's wave equation which couples the light-field to the (optical) interband polarization P and to the (THz) intraband current J . We consider planar structures which can be either a quantum well (QW) or a set of identical quantum wires aligned periodically into a plane with a wire distance much less than the wavelength. In order to compute the dynamic semiconductor response microscopically, we set up the equations of motion for the elementary semiconductor quasi-particle excitations consisting of carriers, phonons, and photons in the formalism of second quantization. The interactions are modeled by the standard Coulomb coupling and the minimal-substitution Hamiltonian.^{6,7} The general properties of a two-band electron-hole system are described by the Fermionic operators $a_{\mathbf{k},c(v)}$ and $a_{\mathbf{k},c(v)}^\dagger$ where, e.g., $a_{\mathbf{k},c(v)}^\dagger$ creates an electron with carrier momentum \mathbf{k} in the conduction (valence) band. Such a system has $P = \frac{1}{S} \sum_{\mathbf{k}} d_{cv}^* P_{\mathbf{k}} + \text{c.c.}$ and $J = \frac{1}{S} \sum_{\mathbf{k},\lambda} [j_{\lambda}(\mathbf{k}) - e^2 A/m_0] f_{\mathbf{k}}^\lambda$ with the normalization area S , microscopic polarization $P_{\mathbf{k}} \equiv \langle a_{\mathbf{k},v}^\dagger a_{\mathbf{k},c} \rangle$, electron $f_{\mathbf{k}}^e \equiv \langle a_{\mathbf{k},c}^\dagger a_{\mathbf{k},c} \rangle$, and hole $f_{\mathbf{k}}^h \equiv \langle a_{\mathbf{k},v} a_{\mathbf{k},v}^\dagger \rangle$ distributions. The vector potential $\mathbf{A}(z, t) = A(z, t) \mathbf{e}_E$ determines the electric field $E(z, t) = -\partial A(z, t)/\partial t$ and its direction \mathbf{e}_E . The corresponding P contains the dipole-matrix element d_{cv} while J depends on the current-matrix element $j_{\lambda}(k) = -|e|\hbar \mathbf{k} \cdot \mathbf{e}_E/m_{\lambda}$ with the effective mass m_{λ} . If the electric field is in the THz regime, the A -dependent part $J_A \equiv -\frac{1}{S} \sum_{\mathbf{k},\lambda} e^2 A/m_0 f_{\mathbf{k}}^\lambda$ of the intraband current and the off-resonant interband P contribute only to the refractive index; together, they provide a Drude-like response if Coulomb interaction is neglected.^{8,9} As a result, $J_{\text{THz}} = \sum_{\mathbf{k},\lambda} j_{\lambda}(\mathbf{k}) f_{\mathbf{k}}^\lambda$ entirely determines the absorption part of the THz response.

In order to compute J_{THz} for the fully interacting system, one has to determine the carrier dynamics

$$\frac{\partial}{\partial t} f_{\mathbf{k}}^e = -\frac{2}{\hbar} \text{Im} \left[P_{\mathbf{k}}^* \Omega_{\mathbf{k}} + \sum_{\mathbf{q},\mathbf{k}'} V_{\mathbf{k}'+\mathbf{q}-\mathbf{k}} c_X^{\mathbf{q},\mathbf{k}',\mathbf{k}} - \sum_{\mathbf{q},\mathbf{k}'} V_{\mathbf{q}} c_{cc}^{\mathbf{q},\mathbf{k}',\mathbf{k}} \right] + \frac{\partial f_{\mathbf{k}}^e}{\partial t} \Big|_{\text{ph}}, \quad (1)$$

where the last term symbolizes the phonon and photon induced contributions. A similar equation holds for $f_{\mathbf{k}}^h$.

Here, $\Omega_{\mathbf{k}} \equiv d_{cv}E(0,t) + \sum_{\mathbf{k}'} V_{\mathbf{k}-\mathbf{k}'} P_{\mathbf{k}'}$ is the renormalized Rabi frequency with the Coulomb matrix element $V_{\mathbf{k}}$. The true two-particle correlations are defined by $c_{\lambda\lambda'}^{\mathbf{q},\mathbf{k}',\mathbf{k}} \equiv \Delta \langle a_{\mathbf{k},\lambda}^\dagger a_{\mathbf{k}',\lambda'}^\dagger a_{\mathbf{k}'+\mathbf{q},\lambda} a_{\mathbf{k}-\mathbf{q},\lambda'} \rangle = \langle a_{\mathbf{k},\lambda}^\dagger a_{\mathbf{k}',\lambda'}^\dagger a_{\mathbf{k}'+\mathbf{q},\lambda} a_{\mathbf{k}-\mathbf{q},\lambda'} \rangle - \langle a_{\mathbf{k},\lambda}^\dagger a_{\mathbf{k}',\lambda'}^\dagger a_{\mathbf{k}'+\mathbf{q},\lambda} a_{\mathbf{k}-\mathbf{q},\lambda'} \rangle_{\text{single}}$ where the factorized single particle contributions are removed to identify excitonic correlation $c_X \equiv c_{cv}$ as well as correlated electrons c_{cc} and holes c_{vv} .

In the THz problem, we solve the two-particle quantities at the same consistent level as the single-particle quantities. More specifically, we use the so-called cluster expansion to identify all lower level particle clusters in general many-body expectation values.^{10,11,12} By keeping all terms up to two-particle clusters exactly and three-particle clusters at the scattering level, the THz dynamics results from

$$i\hbar \frac{\partial}{\partial t} P_{\mathbf{k}} = \tilde{\epsilon}_{\mathbf{k}} P_{\mathbf{k}} + j(\mathbf{k}) A(0,t) P_{\mathbf{k}} - [1 - f_{\mathbf{k}}^e - f_{\mathbf{k}}^h] \Omega_{\mathbf{k}} + \frac{\partial P_{\mathbf{k}}}{\partial t} \Big|_{\text{ph}},$$

$$+ \sum_{\mathbf{k}',\mathbf{l},\lambda} V_{\mathbf{l}} \left[\Delta \langle a_{\mathbf{k},v}^\dagger a_{\mathbf{k}',\lambda}^\dagger a_{\mathbf{k}'+\mathbf{l},\lambda} a_{\mathbf{k}-\mathbf{l},c} \rangle - \Delta \langle a_{\mathbf{k},c}^\dagger a_{\mathbf{k}',\lambda}^\dagger a_{\mathbf{k}'+\mathbf{l},\lambda} a_{\mathbf{k}-\mathbf{l},v} \rangle^* \right], \quad (2)$$

$$i\hbar \frac{\partial}{\partial t} c_X^{\mathbf{q},\mathbf{k}',\mathbf{k}} = \Delta E^{\mathbf{q},\mathbf{k}',\mathbf{k}} c_X^{\mathbf{q},\mathbf{k}',\mathbf{k}} + S^{\mathbf{q},\mathbf{k}',\mathbf{k}} + j(\mathbf{k}' + \mathbf{q} - \mathbf{k}) A(0,t) c_X^{\mathbf{q},\mathbf{k}',\mathbf{k}} + (1 - f_{\mathbf{k}}^e - f_{\mathbf{k}-\mathbf{q}}^h) \sum_{\mathbf{l}} V_{\mathbf{l}-\mathbf{k}} c_X^{\mathbf{q},\mathbf{k}',\mathbf{l}},$$

$$- (1 - f_{\mathbf{k}'+\mathbf{q}}^e - f_{\mathbf{k}'}^h) \sum_{\mathbf{l}} V_{\mathbf{l}-\mathbf{k}} c_X^{\mathbf{q},\mathbf{l},\mathbf{k}} + D_{\text{rest}}^{\mathbf{q},\mathbf{k}',\mathbf{k}} + \gamma_{\mathbf{l},\mathbf{m},\mathbf{n}}^{\mathbf{q},\mathbf{k}',\mathbf{k}} c_X^{\mathbf{l},\mathbf{m},\mathbf{n}}, \quad (3)$$

with the phonon and photon induced correlations $\frac{\partial P_{\mathbf{k}}}{\partial t} \Big|_{\text{ph}}$. The carrier-carrier correlations c_{cc} and c_{vv} obey a similar equation as c_X , however, they do not include the direct THz source proportional to $j(\mathbf{k}) A(0,t) \equiv [j_e(\mathbf{k}) + j_h(\mathbf{k})] A(0,t)$. The different contributions to the c_X dynamics contain the renormalized kinetic energy $\Delta E^{\mathbf{q},\mathbf{k}',\mathbf{k}}$ and the scattering source S which has the typical Coulomb scattering form $V [f_1 f_2 (1 - f_3) (1 - f_4) - (1 - f_1) (1 - f_2) f_3 f_4]$. The explicit summation over V and c_X includes the attractive interaction between correlated electron-hole pairs allowing for the possibility of bound excitons. The remaining two-particle Coulomb and photon contributions are denoted as D_{rest} and the term proportional to γ symbolizes the three-particle Coulomb and phonon terms; all these terms solved in our numerical approach. Equations (1)–(3) together with Maxwell's wave equation present a general description of optical interband as well as intraband THz excitations. When only optical interband fields are applied, the jA -terms can be omitted and Eqs. (1)–(2) reduce to the semiconductor Bloch equations while Eq. (3) describes the formation dynamics of incoherent excitons.^{6,12,13}

In the absence of THz fields, all carrier quantities have even symmetry with respect to a sign change of \mathbf{k} , e.g. $f_{-\mathbf{k}}^\lambda = f_{\mathbf{k}}^\lambda$ while $j_\lambda(\mathbf{k})$ is odd such that $J_{\text{THz}} = \sum_{\mathbf{k},\lambda} j_\lambda(\mathbf{k}) f_{\mathbf{k}}^\lambda = 0$. Finite THz response follows when we subdivide all terms into odd and even quantities via $f_{\mathbf{k},O(E)}^\lambda \equiv [f_{\mathbf{k}}^\lambda \quad f_{-\mathbf{k}}^\lambda]/2$, $P_{\mathbf{k},O(E)} \equiv [P_{\mathbf{k}} \quad P_{-\mathbf{k}}]/2$, and $c_{\lambda\lambda',O(E)}^{\mathbf{q},\mathbf{k}',\mathbf{k}} \equiv [c_{\lambda\lambda'}^{\mathbf{q},\mathbf{k}',\mathbf{k}} \quad c_{\lambda\lambda'}^{-\mathbf{q},-\mathbf{k}',-\mathbf{k}}]/2$. Inserting this general decomposition into Eqs. (2) and (3), we find that, e.g., an odd P_O is driven by $j A P_E$ and an odd $c_{X,O}$ follows from a $j A c_{X,E}$ where j provides the needed symmetry breaking. Once P_O or $c_{X,O}$ are generated, also densities with odd symmetry are created via Eq. (1) and $J_{\text{THz}} = \sum_{\mathbf{k},\lambda} j_\lambda(\mathbf{k}) f_{\mathbf{k},O}^\lambda$ produces a nonvanishing THz response.

In this Letter, we concentrate on the time-resolved linear THz response of a system that has been excited by an optical pulse resonant with band-to-band transitions. The THz field is then applied at different time delays with respect to the optical excitation. The corresponding THz dynamics follows from the odd parts of Eqs. (1)–(3). Besides J_{THz} , also $c_{cc,O}$ and $c_{vv,O}$ are indirectly generated, which leads to the decay of J_{THz} . When J_{THz} is computed from the dynamics of $f_{\mathbf{k},O}^\lambda$, we notice that the coherent $P_{\mathbf{k},O}$ and the incoherent $c_{X,O}$ occur as additive sources in Eq. (1). The THz response from a coherent polarization has already been studied within the framework of the semiconductor Bloch equations.^{14,15} However, when the interband coherences vanish, the nature of the J_{THz} changes since *in the incoherent regime the linear THz response results exclusively from correlated electron-hole pairs*.

In the computations, the single- and two-particle dynamics of Eqs. (1)–(3) contain the bare Coulomb-matrix element while screening originates microscopically from the coupling to the higher order clusters. The three-particle scattering terms γ are approximated to have a statically screened Coulomb interaction formally resulting from coupling to four-particle clusters.^{11,16} In the following, we compute the THz response of a QW and of an array of quantum wires. Because of the demanding numerics, the fully dynamic solution of Eqs. (1)–(3) is evaluated for the quantum wire system; the QW system is solved with for a postulated configuration of excitonic correlations. In both cases, we assume GaAs type parameters; the 3D-Bohr radius is $a_0 = 12.4$ nm and the wire radius is chosen such that the energy separation between the two lowest exciton states is 5 meV. The corresponding 8 nm wide QW has similar excitonic states. At low temperatures and relatively small interband pump excess energies studied here, it is sufficient to include only acoustic phonons¹⁷. The specific forms of the Coulomb and phonon-matrix elements and scattering are discussed in Ref.^{11,12}.

We first apply our THz theory to monitor the build up of correlations after a nonresonant optical pulse excitation where a rapid screening of the bare Coulomb interaction can be expected.^{18,19} Typically, the screened interaction $V_{\mathbf{q}}^S = V_{\mathbf{q}}/\epsilon_L(\omega, \mathbf{q})$ is defined by the longitudinal dielectric function $\epsilon_L(\omega, \mathbf{q})$ with frequency and momentum dependence. In the mean field approximation, $\epsilon_L(\omega, \mathbf{q}) = 1 - \omega_{PL}^2(\mathbf{q})/\omega^2$ such that $1/\epsilon_L$ has a resonance at the plasmon frequency $\omega_{PL}(\mathbf{q})$. The corresponding transversal dielectric function follows from $\epsilon_T(\omega) = 1 + \chi_T(\omega)$ with $\chi_T(\omega) = iJ_{THz}(\omega)/[\omega E_{THz}(\omega)]$.

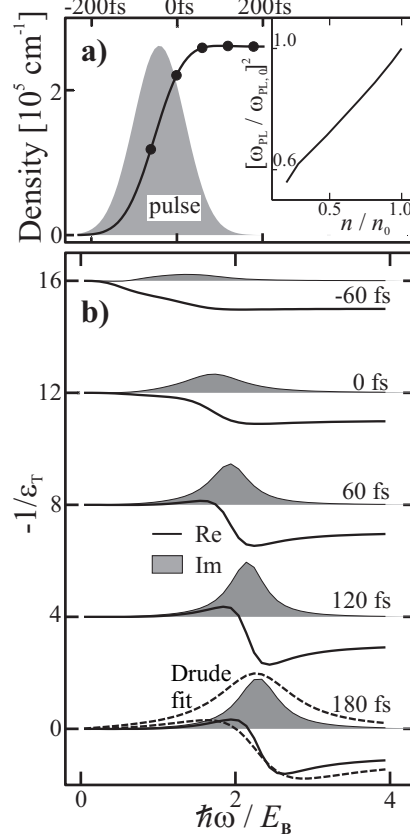


FIG. 1: (a) Time evolution of carrier density (solid line) and exciting pulse $|E|^2$ (shaded area). (b) Real (solid line) and imaginary part (shaded area) of $-1/\epsilon_T$ for different THz probe delays (solid circles in frame above) as function of THz energy ($E_B = 4.2$ meV). Inset shows density dependence of $-1/\epsilon_T$ resonance; n_0 and $\omega_{PL,0}$ correspond to frame (b).

Figure 1 shows the computed time-evolution of $1/\epsilon_T$ for a quantum-wire system that has been excited into the carrier continuum 21 meV above the excitonic resonance with an ultrafast pulse excitation. According to Fig. 1a, a quasi stationary carrier density is built up very quickly and we choose $t = 0$ to correspond to almost fully developed density. Following Ref.⁴, we plot $1/\epsilon_T(\omega)$ in Fig. 1b for the different delay times indicated by the circles in Fig. 1a. For comparison we plot as dashed line a simple Drude response fit, $\chi_{fit}(\omega) = -\omega_{PL}^2/[\omega(\omega + i\delta)]$. Our calculations show that the more or less structureless early time response develops into a clear $1/\epsilon_T(\omega)$ resonance after about 60 fs. This resonance narrows and shifts toward its final position within 180 fs. These dynamical features are very similar to the experimental observations⁴ and the 180 fs response follows from the dynamic build up of Coulomb correlations. The inset to Fig. 1a shows that the computed resonance frequency is proportional to the square root of the density, confirming the basic feature of a plasmon resonance.⁶

At first sight, the observation of a finite plasmon resonance in a QW or quantum-wire system is surprising since a postulated relation $\epsilon_T(\omega) = \epsilon_L(\omega, \mathbf{0}) = 1 - \omega_{PL}^2(\mathbf{0})/\omega^2$ ²¹ predicts $\epsilon_T(\omega) = 1$ because $\omega_{PL}(\mathbf{0})$ vanishes in one- and two-dimensions.⁶ To obtain some insights into the origin of our numerically computed response, we study $\chi_T(\omega)$ when the Coulomb and phonon sums in Eq. (3) are omitted. In this case, $c_{X,O}$ can be solved analytically and the result, inserted into Eq. (1), shows that a part of $S^{\mathbf{q}, \mathbf{k}', \mathbf{k}}$ provides Lindhard-like screening contributions to J_{THz} . We then obtain $\chi_T(\omega) = -\omega^{-2} \sum_{\mathbf{q}} \omega_{PL}^2(\mathbf{q}) S_{\mathbf{q}} = -\omega_{PL}^2(\mathbf{q}_{eff})/\omega^2$ where the Coulomb scattering kernel $S_{\mathbf{q}}$ leads to nonvanishing effective \mathbf{q}_{eff} and $\omega_{PL}(\mathbf{q}_{eff})$. Hence, we identify the Coulomb scattering as relevant source providing a build up of the finite plasmon response.

In comparison to $1/\epsilon_T$, plain ϵ_T may display resonances related to exciton populations.¹³ Following recent

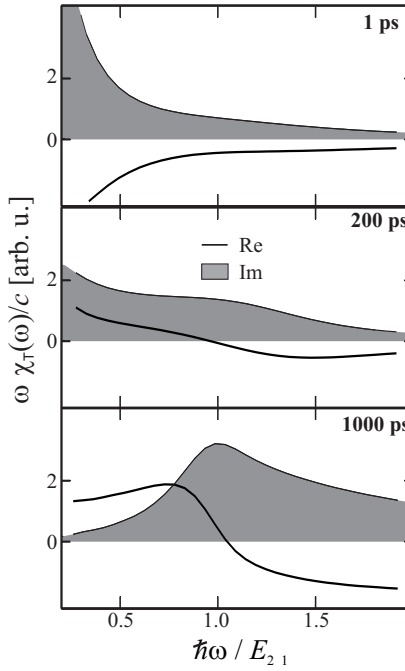


FIG. 2: Terahertz absorption (shaded area) and refractive index change (solid line) for different THz probe delays after nonresonant excitation. Here, $E_{21} = 5$ meV and final density is 6×10^4 cm $^{-1}$.

experiments⁵, we compute THz absorption spectrum $\alpha(\omega) = \omega \text{Im}[\chi_T(\omega)]/c$. As in Fig. 1, the system is nonresonantly excited but we assume a lower excitation intensity and focus on the long time limit to obtain conditions favorable to excitons. Figure 2 shows that the computed $\alpha(\omega)$ is very broad and shows no resonances at 1 ps after the excitation.²⁰ Even after 200 ps, the THz response has changed only moderately due to the slow phonon scattering from electron-hole plasma to excitons. However, roughly 1 ns after the excitation, $\alpha(\omega)$ shows a pronounced resonance at 5 meV corresponding exactly to the energy difference between the two lowest exciton states. At the same time, $\omega \text{Re}[\chi_T(\omega)]/c$ becomes positive for low frequencies in contrast to the 1 ps-response. The asymmetric shape of $\alpha(\omega)$ results from transitions between the lowest and all other exciton states. These results are in good agreement with recent experiments.⁵

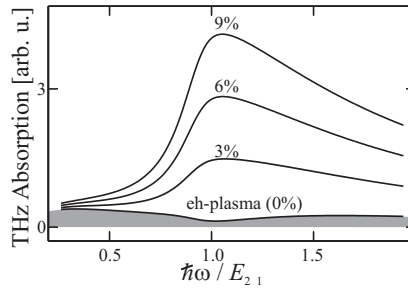


FIG. 3: Terahertz absorption of QW with different postulated exciton fractions. Carrier system at 40 K with density 4×10^9 cm $^{-2}$, and $E_{21} = 7$ meV.

In order to evaluate the THz response of a two-dimensional QW system, we make use of the results published previously.¹² There, a careful analysis of the exciton formation after a band-to-band excitation revealed that the many-body state $c_{X,E}$ corresponding to the late times of Fig. 2 can be accurately described as a superposition of a correlated plasma and a time dependent 1s-exciton population. In Fig. 3 we display the results for such a postulated superposition using different 1s-exciton concentrations. The comparison with Fig. 2 shows that the THz response is qualitatively independent of the dimensions. Furthermore, we observe that the correlated plasma absorption is very much suppressed compared to the result expected from a simplified Drude analysis. Consequently, the transitions from the 1s to the 2p exciton dominate the absorption even for small exciton concentrations.

In summary, a microscopic analysis of the THz response leads to a symmetry breaking where a transversal THz

field generates odd quantities with respect to the carrier momentum. In the incoherent regime, the THz response follows entirely from the correlated electron-hole pairs and can sensitively detect the presence of exciton populations. The computations also demonstrate that the exciton resonance emerges slowly after an off-resonant excitation while the plasmon resonance is built up on an ultrafast time scale even in low-dimensional systems.

Acknowledgments

We thank D.S.Chemla for stimulating discussions about THz experiments. This work was supported by the Deutsche Forschungsgemeinschaft through the Quantum Optics in Semiconductors Research Group, by the Humboldt Foundation and the Max-Planck Society through the Max-Planck Research prize, and by the Optodynamics Center of the Philipps-Universität Marburg.

¹ R.M. Groeneveld and D. Grischkowsky, *J. Opt. Soc. Am. B* **11**, 2502 (1994).
² J. Cerne *et al.*, *Phys. Rev. Lett.* **77**, 1131 (1996).
³ M.C. Beard, G.M. Turner, and C.A. Schmuttenmaer, *Phys. Rev. B* **62**, 15764 (2000)
⁴ R. Huber *et al.*, *Nature* **414**, 286–289 (2001).
⁵ R.A. Kaindl, M.A. Carnahan, D. Hägele, R. Lövenich, and D.S. Chemla, accepted for publication in *Nature* (2003).
⁶ H. Haug and S.W. Koch, *Quantum Theory of the Optical and Electronic Properties of Semiconductors* (World Scientific Publ., Singapore, 1994).
⁷ C. Cohen-Tannoudji, J. Dupont-Roc, and G. Grynberg, *Photons & Atoms*, (Wiley, New York, 1989).
⁸ H. Haug and S. Schmitt-Rink, *Prog. Quantum Electron.* **9**, 3 (1984).
⁹ M. Kira, W. Hoyer, and S.W. Koch, *Phys. Stat. Sol. (b)*, accepted.
¹⁰ J. Fricke, *Ann. Phys.* **252**, 479 (1996).
¹¹ M. Kira, W. Hoyer, and S.W. Koch, *J. Nonlin. Opt. B* **29**, 481 (2002).
¹² W. Hoyer, M. Kira, and S. W. Koch, *Phys. Rev B* **15**, 155113 (2003).
¹³ M. Kira *et al.*, *Phys. Rev. Lett.* **87**, 176401 (2001).
¹⁴ T. Meier *et al.*, *Phys. Rev. Lett.* **73**, 902 (1994).
¹⁵ S. Hughes and D. Citrin, *J. Opt. Soc. Am. B* **17**, 128 (2000).
¹⁶ F. Jahnke, M. Kira, and S.W. Koch *Z. Physik B* **104**, 559 (1997).
¹⁷ A. Thränhardt *et al.*, *Phys. Rev. B* **62**, 2706 (2000).
¹⁸ L. Bányai *et al.*, *Phys. Rev. Lett.* **81**, 882 (1998).
¹⁹ N.-H. Kwong and M. Bonitz, *Phys. Rev. Lett.* **84**, 1768 (2000).
²⁰ The corresponding $1/\epsilon_T$ does show a plasmon resonance in agreement with Fig. 1.
²¹ The momentum of THz photons is practically vanishing at the scale typical for carriers.